JOURNAL OF AIRCRAFT
Vol. 31, No. 5, Sept.-Oct. 1994

Experimental Investigations on Limit Cycle Wing Rock of Slender Wings

Andrew S. Arena Jr.*
Oklahoma State University, Stillwater, Oklahoma 74078
and
Robert C. Nelson†
University of Notre Dame, Notre Dame, Indiana 46556

The phenomena of wing rock of a delta wing with 80-deg sweep has been investigated through a comprehensive series of experiments. Two unique experimental apparatus have been developed for the investigation. A free-to-roll system was developed using an air-bearing spindle that allowed the isolation of applied torques due to the flowfield. An unsteady pressure acquisition system was also developed in order to measure the unsteady surface pressure distributions acting on the wing during wing rock motion. Experimental measurements include motion characteristics obtained from motion history plots, static and dynamic flow visualization of vortex position and vortex breakdown, static surface flow visualization, and steady and unsteady surface pressure distributions. Correlation using the different sources of data provides insight into mechanisms that are most likely to cause the wing rock motion.

Nomenclature

A = wing rock amplitude
b = wing span
C_l = roll moment coefficient
C_l' = roll moment contribution from a single chord station
c_r = root chord
f = frequency, Hz
f_{red} = reduced frequency, (fc_r/V_∞)
I_x = rotational moment of inertia
L = roll moment
L_{aero} = roll moment due to aerodynamic effects
$L_{bearing}$ = roll moment due to bearing friction
q = dynamic pressure
Re = Reynolds number
S = wing area
s = local wing semispan
y_l = left vortex spanwise location
y_r = right vortex spanwise location
z_l = left vortex normal location
z_r = right vortex normal location
α = angle of attack, deg
ΔE = change in energy
ϕ = roll angle, deg

Introduction

WHILE maneuvering at angle of attack many high-performance aircraft can experience a self-induced limit cycle roll oscillation called wing rock. This unwanted motion may result in limitations being placed on the aircraft's flight envelope. The underlying mechanism for the wing rock motion is not clearly understood. Because of the complex geometry of modern aircraft it is difficult to isolate the various flow phenomena created by the forebody, strake, and wing, and their relationship to the wing rock motion. To gain some understanding of the wing rock phenomenon without the complicated interactions between aircraft components, researchers have examined the limit cycle oscillations of simple highly swept, wing alone models.[1-11] Slender flat plate delta wings are known to exhibit a wing rock at angle of attack for low subsonic speeds.

Based on static and dynamic data obtained from the literature, Ericsson[12-15] has developed theories to explain the wing rock motion. Although these theories provide insight into this very complicated dynamic phenomenon, they were not complete due to limitations in the available static and dynamic data.

Nguyen et al.[1] studied the wing rock motion of an 80-deg delta wing through a series of experiments. Their experiments included static force tests, flow visualization, and forced and free-to-roll dynamic experiments. They concluded that the wing rock phenomenon is caused by the dependence of the aerodynamic roll damping on sideslip angle. As a single degree-of-freedom model rolls about its longitudinal axis, the model experiences an effective sideslip. At low sideslip angles the damping is destabilizing, whereas at large sideslip angles the damping is stabilizing. The behavior of the roll damping characteristics was attributed to the effect of sideslip on the strength and position of the vortices as the wing undergoes its rolling motion. Another free-to-roll experiment was conducted by Levin and Katz.[2] They concluded that the wing rock motion was caused by destabilizing vortex interaction that overcame the wing damping forces. Both these studies indicated that the leading-edge vortices played an important role in understanding the wing rock motion. Jun and Nelson[3] studied the behavior of the leading-edge vortices by flow visualization experiments. They used a laser light sheet technique to illuminate the position of the leading-edge vortices above an 80-deg swept delta wing. Both static and dynamic position of the vortices were measured. The dynamic position of the vortices was found to be a function of the direction that the model was rolling, indicating a hysteresis loop in position.

A few experimental studies of the wing rock motion have been conducted in water tunnels.[4,5] Water-tunnel results have revealed large chordwise fluctuations in vortex position, dynamic roll moment hysteresis characteristics, and dynamic roll

Received Jan. 24, 1993; revision received Dec. 21, 1993; accepted for publication Feb. 17, 1994.

*Assistant Professor, School of Mechanical and Aerospace Engineering. Member AIAA.
†Professor, Hessert Center for Aerospace Research, Department of Aerospace and Mechanical Engineering. Associate Fellow AIAA.

moment magnitudes, which all differ greatly from results obtained in wind tunnels. This may be attributable to the very low Reynolds numbers used during the tests (8300–75,000), and relatively high reduced frequencies compared to wind tunnels. Wortman[16] has shown that low-speed water-tunnel data at Reynolds numbers of about 10,000 compare poorly with high Reynolds number turbulent flows as evidenced by the fact that the vortex trajectories were very different, vortex breakdown could not be correlated, and transverse forces not only varied significantly, but were frequently in the opposite direction. Thompson[17] has also shown a difference between vortex trajectories at low and high Reynolds number. As a result of this discrepancy, it is difficult to compare the wing rock results for wind and water tunnels.

In these earlier experiments the free-to-roll apparatus typically consists of a wing connected to a bearing apparatus via a sting. A major problem with this type of free-to-roll experiment is the contamination of the data by bearing friction. Konstadinopolos et al.[6] have shown the significant effect of rotational friction on the limit cycle, using a numerical simulation. Arena and Nelson[7–11] developed a free-to-roll system that was essentially free of mechanical friction. This was accomplished be using an air-bearing spindle. Through a combination of dynamic roll moment measurements and flow visualization experiments they examined the wing rock motion of an 80-deg delta wing. From their results they concluded that a possible mechanism contributing to the destabilizing roll moment necessary to sustain the wing rock motion appears to be the time lag in the position of the vortices normal to the wing surface.

To truly understand the relationship between the vortical flowfield and the unsteady aerodynamic roll moment driving the wing in a wing rock motion, one needs to know information about the surface pressure distributions. A study of the unsteady surface pressure distribution on a slender delta wing during a limit cycle oscillation was also conducted by Arena and Nelson using a unique computer controlled roll drive system.[10,11]

This article outlines the experimental results obtained in studies of the limit cycle wing rock phenomenon by the authors. The investigation consisted of motion history experiments, flow visualization experiments, surface flow visualization, and surface pressure experiments with the goal of identifying the primary fluid mechanisms causing the wing rock behavior.

Experimental Apparatus

The experiments in this study were all performed in the University of Notre Dame low turbulence 2- × 2-ft (61- × 61-cm) subsonic wind tunnel. Two geometrically identical wings were used for these experiments, one for the flow visualization tests and one for the pressure tests. Both wings had a leading-edge sweep of 80 deg, and a root chord of 16.625 in. (42.22 cm). The models were ¼-in.- (0.64-cm-) thick aluminum, resulting in a thickness ratio of 1.5%, and had a 45-deg beveled edge on the bottom leading edges. The models were sting-mounted at the trailing edge with a ⅝-in.- (1.58-cm-) diam steel rod. The sting mount was rotated in angle of attack beneath the tunnel floor such that the trailing edge of the wing always remained 7 in. (17.78 cm) above the tunnel floor. A sketch of the delta wing in the test section may be seen in Fig. 1.

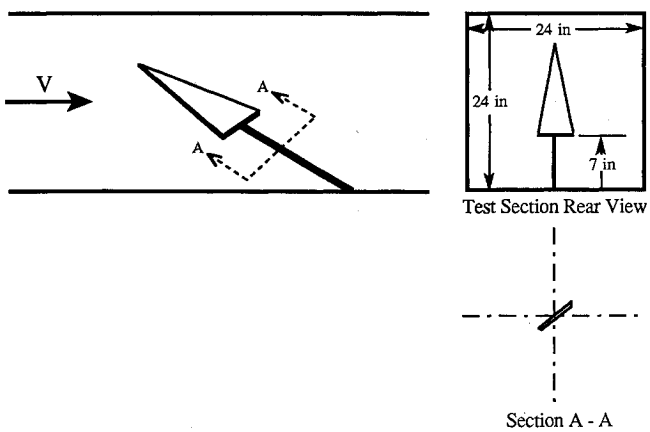

Fig. 1 Sketch showing delta wing, sting, and test section geometry.

Motion history experiments and dynamic flow visualization were accomplished using the specially designed free-to-roll apparatus. Simulation of a single degree-of-freedom free flight environment was accomplished with the use of an air-bearing spindle that significantly reduced the rolling resistance of the free-to-roll apparatus. Experiments revealed that the maximum frictional rolling moment produced with the air bearing was over 90 times less than that produced by conventional bearings. Instantaneous roll angle was measured using a 10-bit optical encoder, yielding a resolution of 0.35 deg. This apparatus was also used to store time history data for use in the motion control system. Flow visualization was accomplished using a kerosene smoke rake to entrain visible particles into the vortices, and a laser light sheet technique to illuminate the leading-edge vortices at a given chord location. A much more in-depth description of the free-to-roll apparatus, model mount, and flow visualization technique may be found in Refs. 7 and 8.

To obtain surface pressure data on a model undergoing wing rock, a unique motion control/data acquisition system was developed. A motion control system was necessary because of the wire leads from the pressure transducers to the data acquisition computer. These leads eliminate the free-to-roll nature of the system. A sketch of the system may be seen in Fig. 2. The pressure model has spanwise pressure taps located at 30, 60, and 90% chord locations on the top and bottom surfaces of the wing. Two pressure transducers are mounted at the trailing edge of the wing, one for each wing half. The transducer leads run from the model to the data acquisition system. The pressure taps are connected to the transducers via a chamber, and all unused taps are sealed by tape. Dynamic tests show no significant attenuation or phase lag of the pressure signal due to the chamber over a range of motions tested.[11]

Motion control is accomplished with a dc servo motor connected to a motor amplifier and motion control computer board. Tachometer and encoder signals are used for feedback. The motion controller uses high-speed digital processing and has an accuracy of ±1 count in 10,000 (0.036 deg). Digital proportional-integral-derivative (PID) with velocity and ac-

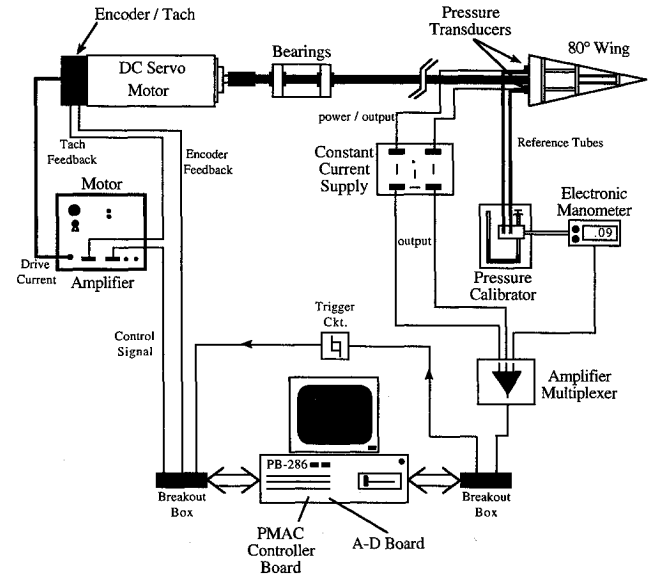

Fig. 2 Unsteady surface pressure acquisition system.

celeration feed-forward control is implemented for precision tracking of the time history. All gains are user adjustable so that the system may be fine-tuned for a given model. The servo motor is connected to the wing via a sting that rides on conventional ball bearings. Time histories taken with the free-to-roll apparatus were used to provide the input signal to the motion control system to drive the model through the wing rock trajectory. The pressure data acquisition system is synchronized with the motion control system so that the roll angle and time is known for each pressure sample.

The motion control system was essential in obtaining the unsteady surface pressure distributions on the delta wing. Instrumenting the model required running pressure transducer leads and reference pressure tubes from the wing to the data acquisition system that eliminates the free-to-roll quality of the experiment. To acquire pressure data on a wing that is undergoing a wing rock motion, it is therefore necessary to match the time-dependent boundary conditions of the controlled wing motion to that of the free-to-roll experiment. In other words, the instrumented model must be driven through the free-to-roll time history. This was accomplished by downloading time history data obtained in the free-to-roll experiments to the motion control system for use as the reference input to be tracked.

Validation of this technique to simulate wing rock was conducted in two steps. First, the roll angle time history was captured from the motor encoder as the instrumented model was being controlled. This time history was compared with the time history obtained from the free-to-roll experiment. It was found that the maximum instantaneous following error between free-to-roll data and controlled motion data was less than 0.5 deg, which is 0.15 deg greater than the resolution of the optical encoder on the free-to-roll apparatus. Tests to examine the repeatability of the controlled motion revealed no discernible difference between runs.

The second validation experiments were concerned with the dynamic behavior of the leading-edge vortices. Flow visualization of vortex core positions were conducted on the free-to-roll model and on the controlled model. Spanwise and normal position of the vortices for each case showed excellent agreement indicating the validity of the technique.[11]

Experimental Results

The Reynolds number used in the present investigation for all experiments was 4×10^5. This Reynolds number was chosen to obtain the maximum signal-to-noise ratio from the transducers for the pressure experiments while not exceeding the cantilever moment limit on the air bearing. The choice of Reynolds number is not critical to obtaining the motion since it was found by Arena and Nelson that the wing rock motion was obtained over the entire Reynolds number range tested between 6×10^4 to 4.75×10^5.[8] Wing rock amplitude and reduced frequency were also found to vary little over this Reynolds number range.

The wing rock dependence on angle-of-attack regime was experimentally determined for the 80-deg wing at a Reynolds number of 4×10^5 (Fig. 3a). The wing would undergo self-induced oscillations when placed at an angle of attack greater than 22 deg. If the model were placed at any initial roll angle for $\alpha \leq 22$ deg, the wing would undergo a lightly damped roll oscillation that would completely decay over a period of time. Angle-of-attack dependence of wing rock amplitude grows rapidly with α until a maximum is reached at approximately 33 deg. Vortex breakdown was not observed on the wing at any time up to and including 36-deg angle of attack. At $\alpha =$ 36 deg, vortex breakdown just reaches the trailing edge of the wing. Note in Fig. 3a the angle-of-attack regime where breakdown exists. Between the angles-of-attack 36 and 40 deg, breakdown appears on the wing in alternating left and right cycles. Above 40 deg, breakdown is seen on both sides of the wing for the entire cycle.

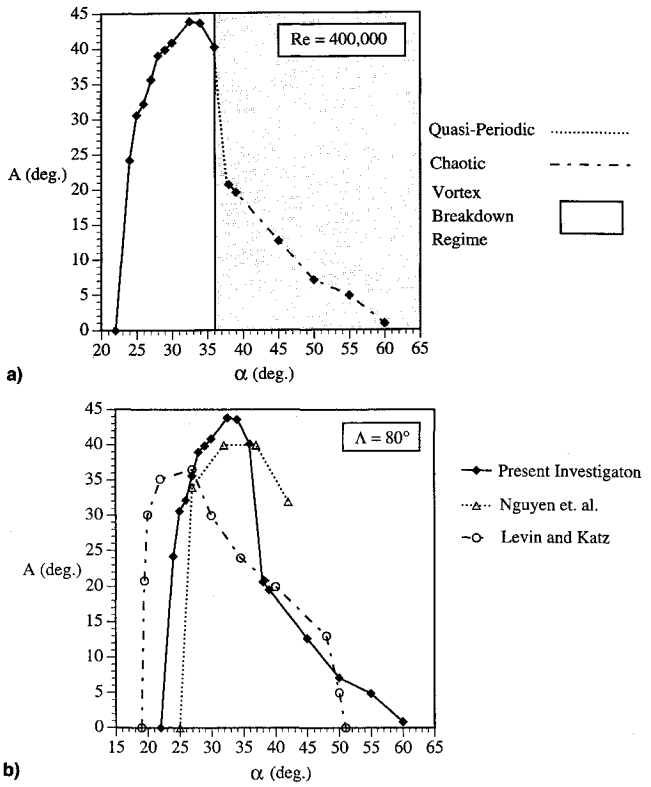

Fig. 3 Wing rock amplitude envelope for the 80-deg wing: a) present investigation and b) comparison with other investigators.

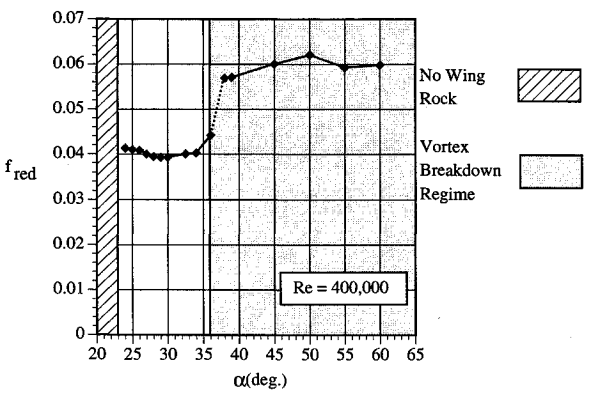

Fig. 4 Dependence of reduced frequency on angle of attack.

Similar wing rock envelopes for the 80-deg delta wing have been obtained by other researchers.[1,2,4] Results from the investigations indicate that after some critical angle of attack is exceeded, wing rock begins. Roll amplitude of the steady state grows rapidly with angle of attack until another critical angle of attack is reached and further increases in angle of attack reduce the amplitude. The angle of wing rock onset obtained by all three investigations are within approximately 6 deg of one another. Levin and Katz observed wing rock above 19 deg and Nguyen et al.[1] observed wing rock above 25 deg (Fig. 3b). Differences are most likely attributable to the different model geometries used, axis of rotation, and most significantly, bearing friction.

Experiments were also conducted to investigate the effect of angle of attack on the frequency of wing rock oscillations (Fig. 4). Once wing rock begins above an angle of attack of 22 deg, the reduced frequency is relatively independent of angle of attack. When vortex breakdown appears on the wing, the frequency jumps to a new level and again remains relatively constant. Results obtained by Nguyen et al. reveal the same type of behavior, however, a quantitative comparison of the data is meaningless since the models were of different

inertia. In the study of Levin and Katz it was observed that reduced frequency moderately increased with angle of attack.

Motion History Results

The wing rock motion was analyzed by obtaining angular velocity and rolling moment information from the roll angle time histories. This information was very useful in studying the limit cycle behavior of the motion. The determination of $\dot{\phi}$ and $\ddot{\phi}$ involved a two-step data reduction process. First, the roll angle time history data was low pass filtered. This was necessary to remove the digital "steps" in the data that would manifest itself as high-frequency noise when differentiated. Central differencing schemes were then used to determine $\dot{\phi}$ and $\ddot{\phi}$. Validation of this method may be found in Refs. 7 and 8.

The calculation of C_l is made simple by the fact that the model is constrained to 1 DOF. The equation of motion for the system is

$$I_x\ddot{\phi}(t) = \sum L(t) \tag{1}$$

where

$$\sum L = L_{\text{aero}} + L_{\text{bearing}}$$

With the use of the air-bearing apparatus, L_{bearing} may be neglected, effectively isolating the aerodynamic effects on the wing. In coefficient form, the equation may be written

$$C_l(t) = [I_x\ddot{\phi}(t)/qSb] \tag{2}$$

Using a torsional pendulum technique, I_x was found to be 8.3×10^{-4} slug-ft^2. With this result, the aerodynamic C_l could then be easily calculated.

With C_l known, the energy exchange technique used by Nguyen et al.[1] was helpful in analyzing the mechanisms driving the limit cycle oscillation. For the single degree-of-freedom motion, the energy is equal to the applied torque times the angular velocity. The energy added to or extracted from the system during the motion for a specific time interval can be expressed as

$$\Delta E = qSb \int_{t_1}^{t_2} C_l(t)\dot{\phi}(t)\, dt \tag{3}$$

This expression for the energy exchange may be written in a more convenient form by rewriting the equation in terms of the instantaneous roll angle $\phi(t)$:

$$\Delta E = qSb \int_{C_\phi} C_l[\phi(t)]\, d\phi \tag{4}$$

where C_ϕ is the curve obtained by plotting C_l as a function of the instantaneous roll angle $\phi(t)$ for a given time interval. The physical interpretation of Eq. (4) is that the energy exchanged in a cycle of motion is directly related to the area enclosed by the rolling moment curve. When the loop encloses an area in a clockwise sense, energy is being added to the system, whereas counterclockwise loops indicate that energy is being dissipated from the system.

A typical wing rock limit cycle time history may be seen in Fig. 5. The wing was released at a 0-deg roll angle and the motion gradually built up to the steady-state amplitude of 40 deg. The time history reveals a characteristic limit cycle behavior.

Figure 6 shows the roll moment coefficient vs roll angle for a typical build-up cycle during the wing rock time history. Note that the clockwise hysteresis loop in the center of the plots completely dominates the damping lobes that are just beginning to form. The roll moment plot indicates that an instability is driving the model towards a divergent behavior,

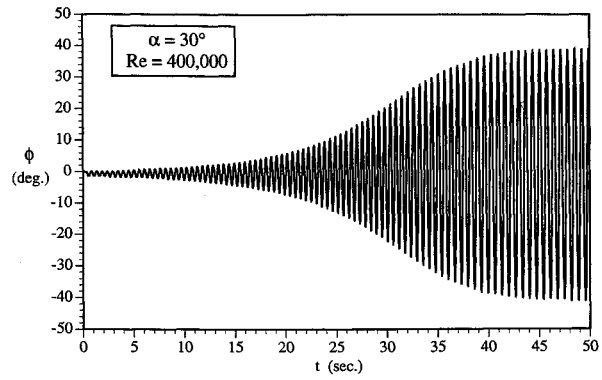

Fig. 5 Wing rock time history for α = 30 deg showing build-up.

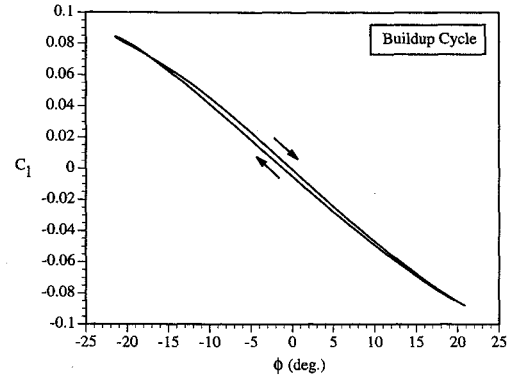

Fig. 6 Roll moment coefficient for a cycle of wing rock build-up.

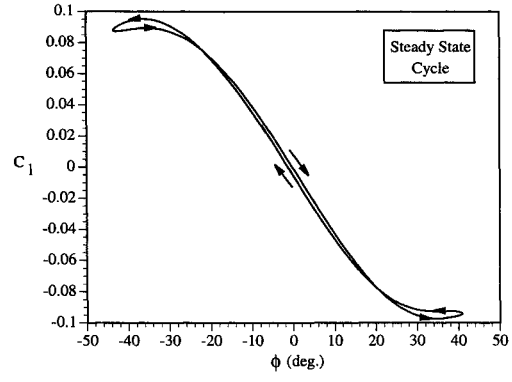

Fig. 7 Roll moment coefficient for a steady-state cycle of wing rock.

hence the build-up cycle. This type of plot is typical throughout the build-up phase of the motion with the damping lobes growing in area as the limit cycle is approached. Also to be noted is that the instability is relatively small, which emphasizes the importance of reducing bearing friction.

Figure 7 is the roll moment coefficient plot for the steady-state cycle of wing rock. It can be seen that the region of instability is roughly equal to the size of the damping lobes. In actuality, the area of the lobes is not equal for every cycle due to small disturbances in the tunnel, and in the model motion itself, however, the time-averaged area of the lobes must be equal to the unstable region for the limit cycle to exist. This roll moment behavior in the steady state is characteristic of the wing rock motion and of many physical phenomena that exhibit limit cycle behavior such as the Van der Pol oscillator. It is not, however, the only type of forcing behavior necessary to generate a limit cycle.

The analysis of time histories, phase planes, and rolling moment plots have revealed a great deal about the behavior of wing rock and the rolling moments that drive the motion. Forced oscillation tests conducted by other researchers on slender wings and aircraft at high angles of attack show a loss of roll damping.[1] The rate-dependent hysteresis characteris-

tics seen in the roll moment plots are the reason for the loss in roll damping, since at certain times in the cycle the roll moment is lagging the model motion. The roll moment plots, however, indicate a necessary condition for the occurrence of wing rock, but do not reveal the aerodynamic mechanisms responsible for the limit cycle oscillation. Mechanisms have been proposed by other researchers as to the cause of wing rock, however, a systematic study of the effect of the flowfield on the motion of the wing had not been conducted. Controversy still remained as to the mechanisms involved. To investigate the mechanisms responsible for the roll moment behavior, experiments were conducted to investigate the behavior of the near and far flowfields, and couple this information with the behavior of the model motion.

Vortex Trajectory Results

It is known that vortex position above a delta wing is a function of roll angle (or sideslip). Jun and Nelson[3] have shown a dependence of vortex position vs roll angle for an 80-deg sweep delta wing experimentally. The results indicate that the static and dynamic vortex trajectories differ greatly. The dynamic position of the vortices exhibits a time lag phenomenon that accounts for the appearance of hysteresis. The vortex position above a delta wing greatly affects the pressure distribution, and it is thought that the movement of the leading-edge vortices may be a driving mechanism in the wing rock motion.

The purpose of these experiments was to correlate the position of the leading-edge vortices with the model motion during wing rock to determine the effect of dynamic vortex movement on the model motion. With the free-to-roll apparatus developed for this study, the vortex position during wing rock could be related to time, roll angle, angular velocity, and rolling moment.

The angle of attack chosen for these experiments was 30 deg. The reason for this choice is twofold. First, since wing rock is present even in the absence of vortex breakdown, the fundamental mechanisms causing the motion can be further isolated by operating at an angle of attack where breakdown is not seen. Secondly, $\alpha = 30$ deg yields large roll excursions, hence, the motion of the vortices are large in amplitude, which reduces the percentage of error when digitizing the video images of the vortices.

Steady vortex experiments were conducted first for a comparison with the unsteady results. Left and right vortex position refers to a view from the trailing edge of the wing. The static results show that as one side of the wing moves downward, its associated vortex moves inward both spanwise and normally, and vice versa on the upward wing. Note that use of the word normal refers to a body fixed coordinate system that rotates with the wing; hence, normal distance is the distance perpendicular to the plane of the wing surface. The positions of the leading-edge vortices were determined as a function of angle of attack and roll angle. The static position data did not show any hysteresis. For the case where the roll angle was zero, the leading-edge vortices remained symmetric as the angle of attack was increased. No vortex position symmetry, i.e., vortex "lift-off," was observed as is commonly seen on slender forebodies. Although vortex position symmetry was maintained, asymmetry in vortex breakdown was observed when breakdown occurred on the wing ($\alpha > 36$ deg). The fact that there is no zero roll angle vortex position asymmetry indicates that wing rock is initiated by some initial perturbation for angles of attack when breakdown is off of the wing. In other words, $\phi = 0$ deg is a dynamically unstable equilibrium point.

Figure 8 is a comparison of spanwise vortex position during 3 cycles of steady-state wing rock to data obtained in the static case at $x/c = 0.9$. No discernible hysteresis loops are seen in the data beyond the scatter. Little difference exists between the static and dynamic data. Hysteresis may be present in the unsteady spanwise data, however, it would be within the uncertainty of the measurement.

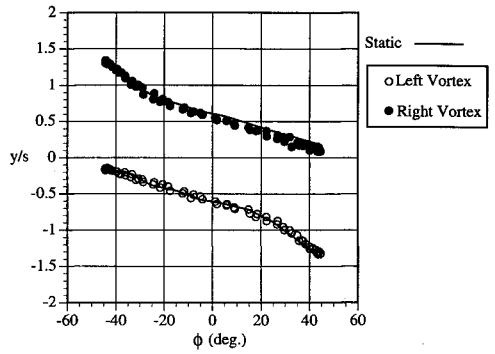

Fig. 8 Spanwise vortex position vs roll angle. $x/c = 0.9$, $\alpha = 30$ deg. Comparison between static roll angle and wing rock.

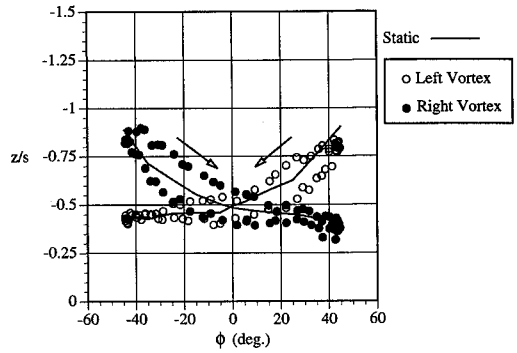

Fig. 9 Normal vortex position vs roll angle. $x/c = 0.9$, $\alpha = 30$ deg. Comparison between static and wing rock.

Figure 9 compares dynamic normal vortex position during wing rock to the static data at $x/c = 0.9$. Large hysteresis loops are apparent in the dynamic data. Arrows are included in the plot to indicate the trajectory of the vortices in time. The hysteresis loops are due to a time lag in the vortex position during the unsteady motion that can clearly be seen by reviewing the videotape of the motion.

The discovery that the vortex position during wing rock lags primarily in the normal sense leads to a hypothesis about the mechanism that may generate wing rock for slender delta wings. In order for wing rock to be sustained, an unstable contribution to rolling moment must be present. The unstable contribution to roll moment is balanced by damping contributions to roll moment in the steady state. A lag in the normal position of the vortices can certainly contribute to an instability by delaying the restoring moment.

Roll moments on the wing are generated from asymmetries in the flowfield. If the flowfield were completely symmetrical about the root chord, no roll moment could exist. Since vortex asymmetries can have such a profound effect on the pressure distribution, it is obvious that a lag in the position of the vortices will contribute differently to the roll moment than one might expect from a static analysis. The effect of the lag in the vortex position on vortex asymmetry during wing rock can be seen more clearly if we define an asymmetry parameter Δz:

$$\Delta z = |z_r| - |z_l| \tag{5}$$

Δz is defined such that for given vortex strengths a positive Δz will contribute to a positive roll moment. Assume that there are no unsteady effects in vortex strength that were considered further in the computational results.[18] It must be kept in mind that this parameter Δz simply gives an indication of qualitatively how normal vortex position asymmetry may affect wing rock. It is most useful when comparing the dy-

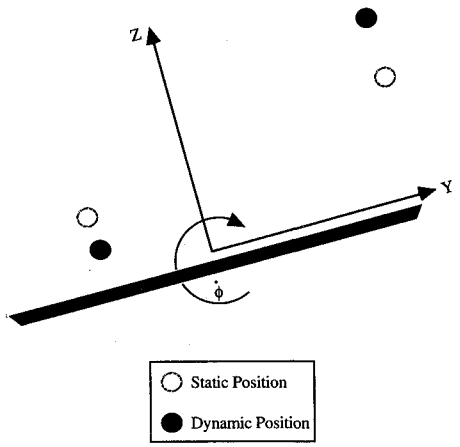

Fig. 10 Sketch of static and dynamic vortex position.

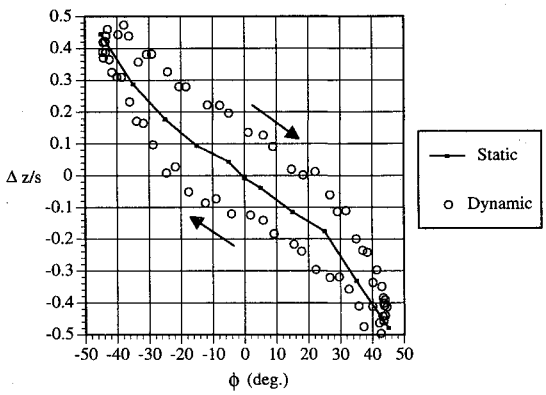

Fig. 11 Vortex asymmetry parameter Δz for three cycles of wing rock.

namic data to the static data. It also cannot be used quantitatively without knowledge of the vortex strength. Figure 10 is a sketch showing static and dynamic vortex asymmetry in the body fixed frame when the wing is at some roll angle ϕ and rolling at a positive roll rate. Note the lag in the normal position of the vortices from the static case. If the strength of the vortices is the same in the dynamic case as in the static case, it can be seen that there is a larger roll moment in the direction of rotation due to the lag in position that will create a dynamic instability. If unsteady vortex strength behavior is present, then the dynamic roll moment will be a function of both contributions from position lag and unsteady strength effects.

Figure 11 shows static and dynamic $\Delta z/s$ for three cycles of steady-state wing rock. The hysteresis is in a clockwise sense that indicates an instability. The shape of the hysteresis is indicative of a rate-dependent hysteresis, since the hysteresis is largest for $\phi = 0$ deg where roll rate is highest, and tapers near the ends. Note that the static asymmetry always favors a restoring contribution to roll moment. The dynamic data shows that due to the lag in asymmetry, the magnitude of the contribution to roll moment is always greater in the direction of rotation than in the static case.

The hysteresis behavior in the normal position of the vortices is the prime candidate for the mechanism responsible for wing rock. The spanwise position of the vortices is seen to differ little from their position during static tests. Assuming that vortex strength does not contribute to an instability in roll moment, the time lag in the normal position of the vortices alone could provide the necessary instability necessary to drive wing rock. Without damping, however, the motion would grow without bound, therefore, there also must be some damping mechanism to balance the instability. Another possible contributor to instability could be unsteady behavior in

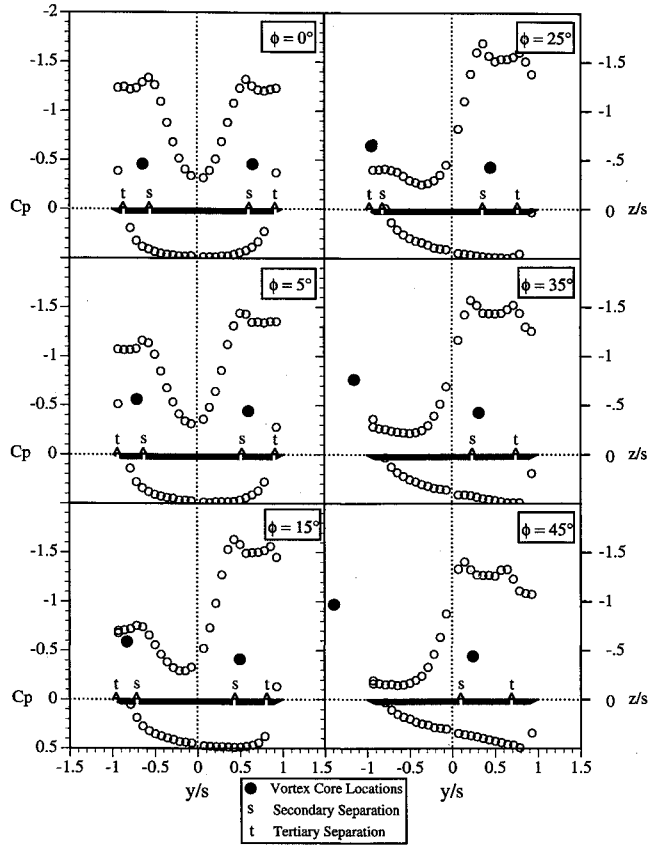

Fig. 12 Correlation of static pressure distributions, surface flow visualization, and vortex position for six positive roll angles (x/c = 0.6, α = 30 deg).

vortex strength. This study could not be done experimentally due to the extremely complicated problem of measuring unsteady vortex strength during wing rock. The role of vortex strength has been analyzed by Arena and Nelson[18] using a simple discrete vortex model. The computational study showed that the unsteady vortex strength provided a damping contribution to the wing. Much more insight into the problem is obtained when the unsteady surface pressures are analyzed.

Surface Pressure Measurements (Static Model)

Static pressure data was taken at three chordwise stations (30, 60, and 90%) for a range of roll angles from −90 to 90 deg. Reynolds number for the tests was 4×10^5, and the angle of attack was 30 deg. Steady surface flow visualization was also conducted. Results of the surface flow visualization may be found in Ref. 11. From the nature of the relatively wide secondary separation regions on the surface of the wing, it was surmised that the surface flow is laminar.

One of the goals of the experimentation was to correlate the vortex position data and the surface flow visualization data with the surface pressure distributions for several roll angles. Figure 12 is a correlation of this data for six positive roll angles. The data is presented at the 60% chord location since the data is qualitatively similar in all other planes. For each roll angle the pressure distribution, left and right vortex locations, and secondary and tertiary separations on the wing surface are seen. As the wing is rolled, the vortex on the downward wing is seen to move downward normally and inboard. The secondary and tertiary separation lines also move inboard and farther apart. The suction peak in the pressure distribution begins to fall off above 25 deg. The opposite trend occurs on the upward side of the wing. The left vortex moves away from the wing and outboard as the pressure peak rapidly falls off. The secondary and tertiary separation lines move outboard and eventually vanish. Notice that even very small movements in the normal sense of the vortex results in large

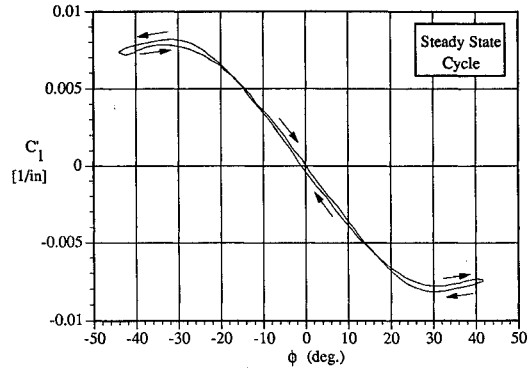

Fig. 13 Sectional roll moment coefficient during a steady-state cycle (x/c = 0.6).

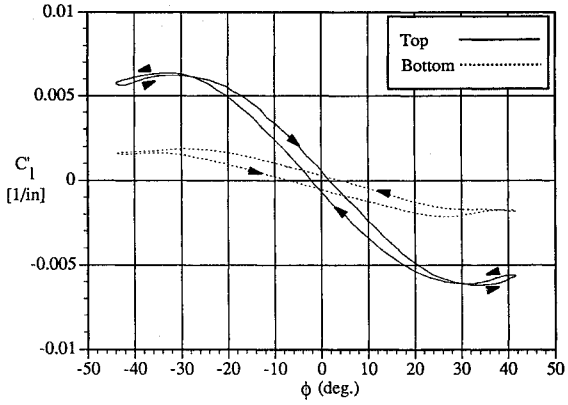

Fig. 14 Sectional roll moment coefficient from top and bottom surfaces (steady state).

changes in the level of the suction peaks. It should be obvious that any time lag behavior in the normal position of the vortices should have a correspondingly large effect on the pressure distribution. The behavior of surface pressure distribution predicts that normal vortex asymmetry will contribute to a restoring moment. Another distinctive feature of the figure is that the suction peak does not lie directly under the spanwise vortex position. Rather, there appears to be two suction peaks, one corresponding with the secondary separation line and one corresponding with the tertiary separation line.

Unsteady Surface Pressure Measurements

The roll moment vs ϕ curves reveal how the limit cycle is sustained during wing rock. However, this roll moment curve is an integrated effect of the surface pressure distributions on the wing. Flow visualization results also reveal a great deal about the behavior of the flowfield on the oscillating wing. However, flow visualization alone cannot quantify how the unsteady flowfield generates the wing rock motion. For these reasons, a study to measure the unsteady surface pressures on a wing undergoing wing rock was conducted.

Unsteady surface pressure data was taken at an angle of attack of 30 deg, and a Reynolds number of 4×10^5, so that the data could be correlated with all of the flow visualization and time history results presented in the previous sections.

To better analyze the unsteady roll moment generated by the surface pressures, the surface pressure distribution at each sampling time interval for the cycle in question was integrated to obtain a C_l', or sectional roll moment. Figure 13 is a plot of C_l' vs roll angle at x/c = 0.6 and for a steady-state cycle of wing rock. The hysteresis behavior is almost identical to that for the actual roll moment on the model obtained from the time history of motion (Fig. 7). A significant discovery was made about the behavior of the unsteady surface pressure when the contribution to roll moment from the top and bottom surface of the wing were analyzed separately. Figure 14 is a plot of both the top and bottom surface contribution to C_l'. The top surface of the wing provides all of the instability to the roll moment as seen by the clockwise sense of the inner hysteresis loop. Beyond approximately $|\phi|$ = 30 deg, the top surface roll moment contribution provides a damping as seen by the counterclockwise damping lobes that limit the amplitude of the wing rock motion. The roll moment contribution from the bottom surface of the wing exhibits the classical rate-dependent hysteresis loop. The loop is in the counterclockwise sense that indicates damping. The damping contribution from the bottom surface is quite large and cannot be neglected when analyzing the roll moment. Without the large damping contribution to the roll moment from the bottom surface the model motion would increase without bound since the size of the damping lobes for the total roll moment would be too small. When a cycle of wing rock during the build-up phase was analyzed it could be seen that the top surface contribution to roll moment was not balanced by the damping from the bottom surface, and the damping lobes were small. The behavior of the integrated rolling moments are consistent with the actual roll moment behavior for each type of cycle (i.e., build-up, steady state, and damping).

Effect of Vortex Breakdown During Wing Rock

Earlier experiments were conducted to ascertain the role of vortex breakdown during wing rock.[7-9] As mentioned previously, vortex breakdown was never observed on the wing during wing rock below an angle of attack of 36 deg. This indicates that vortex breakdown is not a mechanism necessary for the occurrence of wing rock of slender wings. It will, however, modify the motion for angles of attack where it exists.

It was observed that the behavior of vortex breakdown differed greatly between the steady and unsteady cases.[7-9] In the steady case, vortex breakdown contributes an unstable roll moment. In the dynamic case, however, vortex breakdown lags so far behind the model motion that it primarily provides a damping contribution to roll moment. This dynamic effect of breakdown is responsible for the sharp drop in wing rock amplitude for $\alpha > 36$ deg.

Conclusions

A comprehensive experimental investigation has been conducted with an 80-deg swept delta wing at a Reynolds number of 4×10^5 in order to quantify the model behavior and the steady and unsteady flowfield. The experiments revealed a great deal of new information about the wing rock phenomenon.

A range of angle of attack was defined for the 80-deg wing over which wing rock existed. It was found that beyond a critical angle of attack of 22 deg, self-induced oscillations began. Steady-state roll amplitude of the motion increased with angle of attack until another critical angle of attack was reached where further increases in angle of attack reduced amplitude. This angle of attack corresponded with the appearance of vortex breakdown on the wing. No breakdown was seen on the wing at any time during the oscillations between α = 22 and 36 deg, indicating that vortex breakdown is not a necessary condition for wing rock.

Roll moment diagrams were analyzed for several types of wing rock motion including a build-up, steady-state, and damping phase. The roll moment exhibited the characteristic instability and damping lobes seen in other wing rock investigations and for many types of nonlinear dynamical systems that exhibit limit cycle behavior.

Static visualization of vortex core position revealed that the vortex position was a unique function of roll angle. No hysteresis was seen, nor was any zero roll angle asymmetry ever seen. This indicates that a roll angle of 0 deg was an unstable equilibrium point. When the wing was rolled the vortex on the downward wing would move inboard and closer to the

wing, while the vortex on the upward wing would move outboard and away from the wing.

Measurement of vortex position during wing rock revealed a rate-dependent hysteresis. The hysteresis was confined primarily to the motion of the vortices normal to the wing. The hysteresis was due to a time lag in the position. The lag in the position of the vortices has been shown to contribute to a dynamically unstable roll moment that could sustain the wing rock motion.

Steady surface pressure data was taken on the wing at an angle of attack of 30 deg over many positive and negative roll angles from −90 to 90 deg. Distributions were also obtained for three chord stations. Surface pressure data confirmed the surface flow visualization that indicated that the top surface boundary layer was laminar. Changing the roll angle of the wing greatly changed the surface pressure distribution. Contributions to roll moment from the top and bottom surfaces were shown to contribute to a restoring moment for all roll angles tested. The downward wing suction peak increased until a critical roll angle was reached and further increases in roll angle resulted in a decrease of the suction peaks. This behavior can be attributed to the changes in effective angle of attack, effective sweep, and secondary separation.

Surface pressure distributions showed a rate dependency on both the top and bottom surfaces of the wing. All of the instability necessary to generate wing rock can be attributed to the top surface unsteady pressure distributions. The top surface pressure distributions were found to contribute all of the instability that drives wing rock. The top surface also generates the damping lobes, which, when summed with the small damping from the bottom surface, limit the oscillation amplitude. It is likely that these damping lobes are largely due to the unsteady behavior of vortex strength. All of the aerodynamic characteristics necessary to generate wing rock were seen in all three crossflow planes. The behavior of the pressure distributions on the top surface of the wing were consistent with the time lag in normal vortex position.

Acknowledgments

The authors wish to thank Lewis B. Schiff of NASA Ames Research Center for his support and suggestions during the research. Funds for the support of this study have been allocated by the NASA Ames Research Center, Moffett Field, California, under Interchange NCA2-406 and the University of Notre Dame, Notre Dame, Indiana.

References

[1]Nguyen, L. T., Yip, L., and Chambers, J. R., "Self-Induced Wing Rock of Slender Delta Wings," AIAA Paper 81-1883, Aug. 1981.

[2]Levin, D., and Katz, J., "Dynamic Load Measurements with Delta Wings Undergoing Self-Induced Roll Oscillations," *Journal of Aircraft*, Vol. 21, No. 1, 1984, pp. 30–36.

[3]Jun, Y. W., and Nelson, R. C., "Leading Edge Vortex Dynamics on a Delta Wing Undergoing a Wing Rock Motion," AIAA Paper 87-0332, Jan. 1987.

[4]Ng, T. T., Malcolm, G. N., and Lewis, L. C., "Flow Visualization Study of Delta Wings in Wing Rock Motion," AIAA Paper 89-2187, Aug. 1989.

[5]Morris, S. L., and Ward, D. T., "Video-Based Experimental Investigation of Wing Rock," AIAA Paper 89-3349, Aug. 1989.

[6]Konstadinopoulos, P., Mook, D. T., and Nayfeh, A. H., "Subsonic Wing Rock of Slender Delta Wings," *Journal of Aircraft*, Vol. 22, No. 3, 1985, pp. 223–228.

[7]Arena, A. S., Jr., and Nelson, R. C., "The Effect of Asymmetric Vortex Wake Characteristics on a Slender Delta Wing Undergoing Wing Rock Motion," AIAA Paper 89-3348, Aug. 1989.

[8]Arena, A. S., Jr., "An Experimental Study of the Nonlinear Wing Rock Phenomenon," M.S. Thesis, Univ. of Notre Dame, Notre Dame, IN, April 1990.

[9]Arena, A. S., Jr., Nelson R. C., and Schiff, L. B., "An Experimental Study of the Nonlinear Dynamic Phenomenon Known as Wing Rock," AIAA Paper 90-2812, Aug. 1990.

[10]Arena, A. S., Jr., and Nelson, R. C., "Unsteady Surface Pressure Measurements on a Slender Delta Wing Undergoing Limit Cycle Wing Rock," AIAA Paper 91-0434, Jan. 1991.

[11]Arena, A. S., Jr., "An Experimental and Computational Investigation of Slender Wings Undergoing Wing Rock," Ph.D. Dissertation, Univ. of Notre Dame, Notre Dame, IN, April 1992.

[12]Ericsson, L. E., "The Fluid Mechanics of Slender Wing Rock," *Journal of Aircraft*, Vol. 21, No. 5, 1984, pp. 322–328.

[13]Ericsson, L. E., "Analytic Prediction of the Maximum Amplitude of Slender Wing Rock," *Journal of Aircraft*, Vol. 26, No. 1, 1989, pp. 35–39.

[14]Ericsson, L. E., and King, H. H. C., "Rapid Prediction of Slender-Wing Aircraft Dynamics," *Journal of Aircraft*, Vol. 29, No. 1, 1992, pp. 85–92.

[15]Ericsson, L. E., "Slender Wing Rock Revisited," *Journal of Aircraft*, Vol. 30, No. 3, 1993, pp. 352–356.

[16]Wortman, A., "On Reynolds Number Effects in Vortex Flow over Aircraft Wings," AIAA Paper 84-0137, Jan. 1984.

[17]Thompson, D. H., "A Visualization Study of the Vortex Flow Around Double-Delta Wings," Defence Science and Technology Organisation, Aerodynamics Rept. 165, Australia, 1985.

[18]Arena, A. S., Jr., and Nelson, R. C., "A Discrete Vortex Model for Predicting Wing Rock of Slender Wings," AIAA Paper 92-4497, Aug. 1992.